Title

Phylogenomic analysis of *Clostridium perfringens* identifies isogenic strains in gastroenteritis outbreaks, and novel virulence-related features

Running title: Gastroenteritis-associated *Clostridium perfringens*

Author information

Affiliations

Raymond Kiu[1,2], Shabhonam Caim[1], Derek Pickard[3], Anais Painset[4], Craig Swift[4], Gordon Dougan[3], Alison E Mather[5], Corinne Amar[4], Lindsay J Hall[1*]

[1] Gut Microbes & Health, Quadram Institute Bioscience, Norwich, United Kingdom

[2] Norwich Medical School, University of East Anglia, Norwich, United Kingdom

[3] Department of Medicine, University of Cambridge, Cambridge, United Kingdom

[4] Gastrointestinal Bacteria Reference Unit, Public Health England, London, United Kingdom

[5] Microbes in the Food Chain, Quadram Institute Bioscience, Norwich, United Kingdom

Conflict of interest

The authors declare no conflict of interest.

***Corresponding author**

Lindsay J Hall

Lindsay.Hall@quadram.ac.uk

Abstract

Clostridium perfringens is a major enteric pathogen known to cause gastroenteritis in human adults. Although major outbreak cases are frequently reported, limited Whole Genome Sequencing (WGS) based studies have been performed to understand the genomic epidemiology and virulence gene content of *C. perfringens*-associated outbreak strains. We performed both genomic and phylogenetic analysis on 109 *C. perfringens* strains (human and food) isolated from disease cases in England and Wales between 2011-2017. Initial findings highlighted the enhanced discriminatory power of WGS in profiling outbreak *C. perfringens* strains, when compared to the current Public Health England referencing laboratory technique of Fluorescent Amplified Fragment Length Polymorphism (fAFLP). Further analysis identified that isogenic *C. perfringens* strains were associated with nine distinct care home-associated outbreaks over the course of a 5-year interval, indicating a potential common source linked to these outbreaks or transmission over time and space. As expected the enterotoxin CPE gene was encoded in all but 4 isolates (96.4%; 105/109), with virulence plasmids encoding *cpe* (particularly pCPF5603- and pCPF4969-family plasmids) extensively distributed (82.6%;90/109). Genes encoding accessory virulence factors, such as beta-2 toxin, were commonly detected (46.7%; 50/109), and genes encoding phage proteins were also frequently identified, with additional analysis indicating their contribution to increased virulence determinants within the genomes of gastroenteritis-associated *C. perfringens*. Overall this large-scale genomic study of gastroenteritis-associated *C. perfringens* suggested that 3 major sub-types underlie these outbreaks: strains carrying (1) pCPF5603 plasmid, (2) pCPF4969 plasmid, and (3) strains carrying *cpe* on transposable element Tn*5565* (usually

integrated into chromosome). Our findings indicate that further studies will be required to fully probe this enteric pathogen, particularly in relation to developing intervention and prevention strategies to reduce food poisoning disease burden in vulnerable patients, such as the elderly.

Introduction

Clostridium perfringens is an important pathogen known to cause disease in humans and animals (1, 2). Notably, the pathogenesis of *C. perfringens*-associated infections is largely attributed to the wide array of toxins this species can produce, with >20 toxins currently identified (3, 4). This Gram-positive spore former has been associated with foodborne and non-foodborne diarrhoeal diseases in humans, and preterm-necrotising enterocolitis (5, 6).

C. perfringens-associated food poisoning, also termed acute watery diarrhoea, was first documented in the UK and USA in the 1940s (7). Typical symptoms occur within 8-14 h after ingestion of food contaminated with at least 10^6 CFU/g of live bacterial cells. These include intestinal cramp, watery diarrhoea without fever or vomiting, which normally resolves in 12-24 h (8). Importantly, *C. perfringens* is currently the second most common foodborne pathogen in the UK after *Campylobacter*, with cases often under reported due to the frequently self-limiting nature of the illness, with current estimates suggesting ~80,000 cases/annum (9-12).

In the UK, antibiotic-associated diarrhoea and non-foodborne outbreaks of *C. perfringens* diarrhoea have been frequently reported since the 1980s amongst the elderly, particularly in hospital settings (13). With this type of illness, symptoms are more severe than foodborne diarrhoea and are longer lasting (>3 days to several weeks), often chronic, and infections are more likely to be spread amongst cases (14). This type of *C. perfringens* infection has also

been reported in elderly patients, especially those residing in care homes in the North East of England between 2012-2014 (83% of the outbreaks reported from care homes) (10). Although fatality due to *C. perfringens* diarrhoea is uncommon and hospitalisation rate is low, enterotoxigenic *C. perfringens* is reported to cause ~55 deaths/year in England and Wales according to the UK Food Standards Agency (15, 16).

The newly expanded and revised toxinotyping scheme classifies *C. perfringens* into 7 toxinotypes (type A-G) according to the combination of typing toxins produced, with this classification used in this article (17). Human cases of *C. perfringens* diarrhoea are primarily caused by type F strains (formerly classified as enterotoxigenic type A), which produce enterotoxin (CPE), encoded by the *cpe* gene (18). This potent pore-forming toxin is reported to disrupt intestinal tight junction barriers, which is associated with intestinal disease symptoms (19). *C. perfringens*, and associated encoded toxins, have been extensively studied with respect to disease pathogenesis, with a strong focus on animal infections (20-24). Recent studies analysing a range of diverse *C. perfringens* strains (from both animal and human-associated infections) indicates a plastic and divergent pangenome, with a significant proportion of accessory genes predicted to be involved in virulence mechanisms and metabolisms, linked to enhanced host colonisation and disease initiation (3, 25). However, studies describing human outbreak-associated *C. perfringens* infections are limited, and to date only one recent study (58 isolates) has utilised Whole Genome Sequencing (WGS) data to probe the genomic epidemiology of associated strains (3, 26).

We have applied in-depth genomics and phylogenetic analyses to whole genome sequences of 109 newly-sequenced *C. perfringens* isolates associated with outbreaks or incidents of *C. perfringens* diarrhoea in England and Wales, either foodborne or non-foodborne-derived. We also identified distribution of known virulence-related determinants including toxin and antimicrobial resistance (AMR) genes, virulence-associated plasmid contents within food and

95 case isolates and probed putative functional capabilities of the accessory genomes and
96 virulence features within encoded phage genomes. Importantly, we determined that isogenic
97 strains were associated with 9 care-home outbreaks in North East England between 2013-
98 2017, and furthermore uncovered the significant involvement of virulence plasmid-carrying
99 *C. perfringens* in these outbreaks.

100

101 ## Materials and methods

102 **Bacterial isolates, PCR and genomic DNA extraction**

103 *C. perfringens* isolated from clinical cases of diarrhoea and suspected foods when available,
104 were referred to the reference laboratory at PHE, Gastrointestinal Bacteria Reference Unit
105 (GBRU). Identification and characterisation of cultures was performed by detection of the *C.*
106 *perfringens* alpha toxin and enterotoxin gene by duplex real time PCR as described elsewhere
107 (27). Enterotoxigenic *C. perfringens,* when associated with an outbreak or incident, were then
108 further typed for strain discrimination using fluorescent amplified fragment length
109 polymorphism (fAFLP) as previously described (28). In this study, 109 cultures
110 characterised and archived by the GBRU between 2011 and 2017 were selected, representing
111 enterotoxigenic and non-enterotoxigenic isolates from sporadic cases and outbreaks of *C.*
112 *perfringens* food poisoning and of non-foodborne *C. perfringens* diarrhoea (**Table S1**).

113 DNA was extracted from overnight *C. perfringens* cultures (maximum of 1 x 10^7cells) lysed
114 with lysis buffer (200µl Qiagen Buffer P1, 20 µl lysozyme with concentration at 100mg/ml)
115 and incubated at 37^{o}C for 1 h before addition of 20 µl Proteinase K (QIAsymphony DSP
116 DNA kit), and incubation at 56^{o}C for 5 h until cells had visibly lysed. Following incubation at
117 96°C for 10 min, to inactivate proteases and any viable cells remaining, RNA was removed
118 by adding 0.4 mg of RNAse (Qiagen, Manchester) and incubation at 37^{o}C for 15 min.

Genomic DNA was then purified using the QIAsymphony DSP DNA kit on a QIAsymphony SP automated DNA extraction platform (Qiagen, Manchester) according to manufacturer instructions.

Computing infrastructure

Computational analyses were performed on Norwich Biosciences Institute's (NBI) High Performing Computing cluster running Linux CentOS v7. Open-source software was utilised for genomic analysis.

Genomic DNA sequencing

Pure bacterial DNA was subjected to standard Illumina library preparation protocol prior to sequencing on in-house Illumina MiSeq (PH091-PH156) or HiSeq 2500 platforms (PH004-PH090; at Wellcome Trust Sanger Institute, UK) with read length (paired-end reads) 2 x 101 bp and 2 x 151 bp respectively.

Genome assembly and annotation

Sequencing reads were assembled using SPAdes v3.11 (PH091-PH156) to generate draft genomes, the remaining assemblies were generated at Wellcome Trust Sanger Institute (Hinxton, UK) as described previously (for assembly quality see **Table S2**)(29, 30). Assemblies were improved by scaffolding/gap filling using SSPACE v3.0 and GapFiller v1.10 (31-33). Sequencing reads and coverage counts were calculated via in-house custom script using FASTQ reads and FASTA assemblies. Genome assemblies were annotated by Prokka v1.13 using in-house Genus-specific database that included 35 *Clostridium* species retrieved from NCBI RefSeq database to construct genus-specific annotation database (**Table S3**)(34). Sequences from very small contigs (contig size <200 bp) were removed prior to coding region prediction. Assembly statistics were extracted from Prokka outputs using an in-house script. Draft genomes were checked for sequence contamination using Kraken v1.1

(based on MiniKraken database) (35). All draft genomes containing >5% of contaminated species sequences (other than *C. perfringens*), whole genome Average Nucleotide Identity (ANI) < 95% (compared with reference genome NCTC8239; performed with Python module pyani v0.2.4), and assemblies with >500 contigs (considered as poor assemblies) were all excluded from further study (n=21)(36).

Reference genome

A newly sequenced historical foodborne isolate genome NCTC8239 under the NCTC3000 project[1] was retrieved (accession: SAMEA4063013) and assembled in this study with Canu pipeline v1.6 using PacBio reads (37). The final high-quality assembled genome consists of 3 008 497 bp in 2 contigs (contig 1 has 2 940 812 bp, contig 2 has 67 685 bp).

Pangenome and phylogenetic analyses

Pangenome of isolates was constructed using Roary v3.8.0 at BLASTp 90% identity, adding option -s (do not split paralogs), and options -e and -n to generate core gene alignment using MAFFT v7.3 (38, 39). Roary took GFF3-format annotated assemblies generated by Prokka. The pangenome includes both the core and accessory genomes; core genome is defined as genes present in at least 99% of the genomes, accessory genome as genes present in <99% of the genomes. SNP-sites v2.3.3 was used to extract single nucleotide variants from the core gene alignment for re-constructing a phylogenetic tree (40). Phylogenetic trees were generated using FastTree v2.1.9 and annotated using iTOL v4.2 (41, 42). FastTree was run using the Generalized Time-Reversible (GTR) model of nucleotide evolution on 1000 bootstrap replicates to generate maximum-likelihood trees (41). SNP distance between genomes were computed using snp-dists (43). Population structure was analysed via the Bayesian-based clustering algorithm hierBAPS to assign lineages, implemented in R using

[1] https://www.sanger.ac.uk/resources/downloads/bacteria/nctc/

rhierbaps v1.0.1 (44, 45). The pangenome was visualised in Phandango while plots were generated using the associated R scripts in the Roary package (46).

Profiling virulence and plasmid-related sequences

Screening of toxin and AMR gene profiles, IS elements and plasmid *tcp* loci were performed via ABRicate with 90% identity and 90% coverage minimum cutoffs to infer identical genes based on a custom toxin database and the CARD database v2.0.0 (AMR) as described previously (47, 48). ARIBA v2.8.1 was used as a secondary approach to confirm detections of both toxin and AMR genes in raw sequence FASTQ files (49). Heat maps were generated in R using *gplots* and function *heatmap.2* (50, 51).

***In silico* plasmid analysis**

Sequencing reads were utilised for computational plasmid prediction via software PlasmidSeeker v1.0 (52). Plasmid prediction was based on 8 514 plasmid sequences available in NCBI Reference Sequence databases (RefSeq; including 35 *C. perfringens* plasmids, see **Table S4**). All reads were searched for matching k-mers at k-mer length of 20 and screening cutoff at P-value 0.05 based on FASTQ reads. The top predicted plasmids appearing in each 'cluster' (with highest k-mer identity; k-mer percentage ≥80% as the minimum cutoff) were extracted as predicted plasmids (**Table S5**). Binary heat maps were generated as described in the previous section. Plasmid sequences from high-sequencing-coverage assemblies (>200X; single contig; n=12) were extracted using in-house Perl scripts, identified by plasmid gene content. Plasmid annotation was performed via Prokka v1.13 using *Clostridium* genus-specific database as described in the previous section. Plasmid comparison and visualisation were performed using Easyfig v2.2.2.

188 **Bacterial genome-wide association analysis**

189 To associate subsets of genes with specific outbreaks or isolates, we used Scoary v1.6 to
190 identify statistically-related genes based on Roary output (53). Cutoffs were set as ≥80%
191 sensitivity and 100% specificity. Specifically, for a Care Home (CH) and Food Poisoning
192 (FP) subset comparison, sensitivity cutoff was set at ≥50% and specificity at 100%.

193 **Pangenome-wide functional annotation**

194 Functional categories (COG category) were assigned to genes for biological interpretation via
195 eggNOG-mapper v0.99.3 based on the EggNog database (bacteria) (54, 55). Genes of interest
196 were extracted via in-house Perl scripts from Roary-generated pangenome references.
197 Annotations and COG categories were parsed with in-house scripts. Bar plots were generated
198 using GraphPad Prism v6.

199 **Prophage mining**

200 Web tool PHASTER was utilised for detection of intact prophage existing in bacterial
201 genomes (**Table S6**). Annotated GenBank files were submitted manually to the PHASTER
202 web server and annotated data parsed with in-house scripts. The detection of phage was based
203 on the scoring method and classification as described previously (56). Only intact phage
204 regions within the genomes of completeness score >100 (of maximum 150) were analysed
205 further (extracted by default using PHASTER web tool), annotated and colour-coded using
206 Prokka v1.13 and Artemis for visualisation in EasyFig v2.2.2 and R package *gplots* function
207 *heatmap.2* (57, 58). Bar plots were generated using GraphPad Prism v6.

208 **Nucleotide sequence accession numbers**

209 Sequence data in this study will be submitted to the European Nucleotide Archive (ENA) and
210 made available under accession PRJEB25764 upon acceptance of manuscript.

211

Results

Whole-genome based phylogenetic analysis reveals potential epidemiological clusters

Initially we analysed the population structure of all strains sequenced. We defined general food poisoning isolates as Food Poisoning (FP, n =74), and care home specific isolates as Care Home (CH, n =35) (**Fig. 1A-B**). Quality of the genomic assemblies of draft genomes was also determined (**Fig. 1C; Table S2**), with >70% of the isolate assemblies <200 contigs.

Separate analysis of CH isolates indicated four distinct phylogenetic lineages relating to care home outbreaks (**Fig. 2A**). Lineage I contained the reference genome NCTC8239, a historical *cpe*-positive isolate (originally isolated from salt beef) associated with a FP outbreak, and three newly sequenced strains (7). The remaining isolates clustered within three lineages (i.e. II, III and IV), that were divergent from lineage I indicating these CH isolates might be genetically distinct from typical FP isolates as in **Fig. 1A**. Further analysis indicated that 18 closely-related strains obtained from 9 different outbreaks between 2013-2017 which occurred in the North East England, clustered within the same IVc sub-lineage (**Fig. 2B**). SNP investigation on these IVc isolates determined within-sub-lineage pairwise genetic distances of <80 SNPs (29.9 ± 16.6 SNPs; mean ± S.D.**; Table S7**), suggesting a close epidemiological link. Isolates associated with specific outbreaks within sub-lineage IVc (i.e. outbreaks 2, 7, 8, 9 and 10) showed very narrow pairwise genetic distances <20 SNPs (6.6 ± 6.6 SNPs; mean ± S.D.; **Fig. 2C**), suggesting potential involvement of an isogenic strain (genetically highly similar) within these individual care home outbreaks (although a number of genetically dissimilar strains were also isolated from outbreaks 1, 2, 3, 6, 7 and 8 as shown in **Fig. 2A**).

This WGS analysis was also shown to have greater discriminatory power than the currently used fAFLP. The fAFLP typing (type CLP 63, yellow-coded) failed to discriminate isolates

from 6 different outbreaks (CH outbreaks 2-7; **Fig. 2A**), while SNP analysis clearly distinguished these strains (**Fig. 2B**) (59).

Analysis of FP isolates indicated clear separation between linages (**Fig. 3A**), particularly between lineage I, and remaining lineages II-VII (pairwise mean SNP distance lineage I vs lineages II-VII: 35165 ± 492 SNPs; within lineage I: 5684 ± 2498 SNPs; within lineages II-VII: 13542 ± 8675 SNPs). Isolates from three individual foodborne-outbreaks within lineage VII appear to be highly similar even though these isolates demonstrated geographical heterogeneity (**Fig. 3A**), and further analysis indicated two different outbreaks that occurred in London (2013) were related, but somewhat distinct from isolates obtained in North East England (2015) outbreaks (**Fig. 3B**). This suggests a geographical separation of a common ancestor at an earlier time point and may also indicate the potential widespread distribution of a genetically-related strain.

Isolates from individual FP outbreaks also appeared to be clonal and isogenic, as pairwise genetic distances were between 0-21 SNPs (mean genetic distance: 2.6 ± 2.7 SNPs; **Fig. 3C and Table S8**), when compared to same-lineage-between-outbreaks SNP distances of >1200 SNPs (**Fig. 3D**). In addition, outbreak-associated food source isolates were not distinguishable from human clinical isolates (genetically similar, pair-wise SNP range: 0-16 SNPs) in 7 individual FP outbreaks (**Fig. 3A**). These findings are consistent with the hypothesis that contaminated food is the main source of these *C. perfringens* food poisoning outbreaks, which included all meat-based food stuffs e.g. cooked sliced beef, lamb, chicken curry, cooked turkey and cooked meat (**Table S1**).

Virulence gene content

Diarrhoea symptoms associated with *C. perfringens* are primarily due to production of the pore-forming toxin enterotoxin (CPE) by *C. perfringens* type F strains (2, 60). Additional

virulence determinants implicated in diarrhoea include sialidase (NanI), which is linked to enhanced intestinal attachment and an accessory role in enhancing CPE cell-toxicity, and also pore-forming toxin perfringolysin (PFO), a toxin known to act synergistically with alpha-toxin (phospholipase produced by all *C. perfringens* strains) to inflict intestinal cell damage (24, 61, 62). Moreover, antibiotic-resistant *C. perfringens* are reported to be prevalent, particularly within poultry, thus antimicrobial resistance (AMR) profiles of *C. perfringens* may be linked with prolonged *C. perfringens* associated-infections, and may hamper downstream treatments strategies (63, 64). To probe these important virulence-associated traits we screened isolates for toxin and AMR genes, based on both genome assemblies and raw sequence reads.

Enterotoxin gene *cpe* was detected in all, but 4 isolates (PH017, PH029, PH045 and PH156 were *cpe*-negative), which was confirmed by PCR, with the exception of PH029 which was initially determined to be *cpe*-positive via PCR (96.4%; **Table S1**; **Fig. S1B**).

CH isolates (average 9.6 ± 1.0 toxin genes per isolate) encoded significantly more toxin genes ($P<0.001$) than FP isolates (7.3 ± 1.9 toxin genes per isolate; **Fig. S1A**). CH isolates in lineages II-IV generally possessed identical toxin profiles (**Fig. 4A**); colonisation-related sialidase-encoding genes *nanI*, *nanJ* and *nagH*, haemolysin PFO gene *pfo*, and *cpb2* (**Fig. S1C-G**), which produces a vital accessory toxin beta-2 toxin (CPB2) associated with CPE-mediated pathogenesis (65). However, CH isolates did not harbour many acquired AMR genes; only 6 isolates (out of 35; 17%) encoded tetracycline resistant genes *tet(P)*, one isolate encoded aminoglycoside resistant gene *APH(3')*, with remaining isolates not encoding any acquired AMR genes, other than the intrinsic AMR gene *mprF*.

FP isolates had a more variable virulence gene profile (**Fig. 4B**). Isolates in lineage I had identical toxin genes, including *cpe*, but these isolates did not encode toxins such as PFO,

CPB2 and sialidase NanI, and only three isolates in this lineage carried tetracycline resistant genes (19%). Most isolates within lineages II-VII (92%; 53/58) encoded *tetA(P)*, with this AMR gene significantly enriched in all FP isolates (74.3%; 55/74; P<0.0001; **Fig. S1H**), when compared to CH isolates (17.1%; 6/35). Furthermore, most isolates in FP lineages II-VII also encoded toxin genes *cpe*, *nanI* and *pfo*, and 16 isolates (28%) possessed the accessory toxin gene *cpb2*. Statistically these FP isolates (8.0 ± 1.5 toxin genes) encoded more toxin genes than those belonging to FP lineage I (4.9 ± 0.3 toxin genes; P<0.0001; **Fig. S1I**) which may suggest increased virulence. Initial plasmid detection indicated that virulence plasmid pCPF5603 was associated with CH isolates (97% in CH plasmid-carrying isolates; 34/35; P<0.0001), while plasmid pCPF4969 was linked to FP isolates (86.4% in FP plasmid-carrying isolates; 51/59; P<0.0001; **Fig. S1J**).

Specific plasmid-associated lineages and potential CPE-plasmid transmission

The CPE toxin is responsible for the symptoms of diarrhoea in food poisoning, and non-foodborne illnesses, in the latter usually lasting >3 days, and up to several weeks (2, 66). Genetically, whilst chromosomal encoded *cpe* strains are primarily linked to food-poisoning (67, 68), non-foodborne diarrhoea is usually associated with plasmid-borne *cpe* strains (66, 69, 70). We performed an in-depth plasmid prediction on our datasets and analysis indicated that CH isolates predominantly harboured pCPF5603 plasmids (34/35 isolates; 97%) encoding *cpb2* and *cpe* genes, whilst FP isolates carried primarily pCPF4969 plasmids (45/75 isolates; 60%) encoding *cpe* but not *cpb2* genes (**Fig. S1J**). We also performed a genome-wide plasmid-specific sequence search to confirm our findings including IS*1151* (pCPF5603), IS*1470*-like (pCPF4969) and plasmid conjugative system *tcp* genes (**Fig. 4A-B)** (71-73).

To further examine and confirm the predicted plasmids, we extracted plasmid sequences (complete unassembled single contig) from three isolates per CH or FP group, and compared

309 with reference plasmids (**Fig. 5A-C**). The extracted plasmid sequences closely resembled the
310 respective reference plasmids, with near-identical nucleotide identity (>99.0%), plasmid size
311 and GC content (**Fig. 5B-C; Table S9**), thus supporting the findings that these two intact
312 plasmids (pCPF4969 and pCPF5603) are present in these isolates.

313 Although chromosomal-*cpe* strains are considered as the primary strain type to be associated
314 with food poisoning, our dataset demonstrated that plasmid-*cpe C. perfringens* strains were
315 predominantly associated with food poisoning (82.6%; 90/109), with only 17.4% FP isolates
316 encoding a copy of *cpe* on the chromosome (no plasmid detected). Putatively, plasmid
317 transfer may have occurred in CH outbreak 7 isolates (n=4; PH030, PH031, PH032, PH033),
318 as two isolates reside within lineage IV, whilst the other two isolates nest within the
319 genetically distant CH lineage I (genetic distance >10 000 SNPs), however all 4 isolates
320 harboured plasmid pCPF5603 (**Fig. 4A**). CH outbreaks 1 and 8 also had dissimilar strains
321 (nested within separate lineages) with identical plasmids. This analysis denotes that multiple
322 distinct strains, but carrying the same *cpe*-plasmid, may be implicated in these CH outbreaks,
323 with previous work showing *in vitro* plasmid transfer among *C. perfringens* strains via
324 conjugation (*cpe*-positive to *cpe*-negative strains) (74).

325 Previous studies have demonstrated that *C. perfringens* with chromosomally-encoded *cpe* are
326 genetically divergent from plasmid-*cpe* carriers. Within the FP phylogeny there was a distinct
327 lineage of isolates (lineage I; n=17) that appear to encode *cpe* chromosomally. These isolates
328 had significantly smaller genomes (genome size 2.95 ± 0.03 Mb vs 3.39 ± 0.08 Mb outside-
329 lineage; n=93; P<0.0001; **Table S10**), were most similar to reference genome NCTC8239
330 (ANI≥99.40%) and appeared to lack plasmids. This was further evidenced by historical
331 chromosomal-*cpe* strain NCTC8239 nesting in this lineage with these newly sequenced
332 strains (FP lineage I; **Fig. 4**) (70, 72, 75). To further investigate this hypothesis, the *cpe*-
333 encoding region (complete single contig from high-coverage assemblies) was extracted from

representative isolates in lineage I (n=6), and comparative genomics was performed (**Fig. 5D**). These consistently smaller (~4.0-4.3 kb) contigs were almost identical in nucleotide identity (>99.9%) when compared with the *cpe*-encoding region of chromosomal-*cpe* strain NCTC8239, confirming that these isolates possessed the same *cpe* genomic architecture as NCTC8239 and confirmed as transposable element Tn*5565* (**Fig. 5E**). In addition, PH029 was the only outbreak isolate not detected to encode *cpe* within the lineage I outbreak cluster, despite having a clonal relationship with PH028, PH104, PH105 and PH107 (FP outbreak 4; **Fig. 4B)**. This suggests Tn*5565* loss may have occurred due to extensive sub-culturing (this is supported by initial PCR results being *cpe*-positive; see **Table S1**). Analysis also indicates that *cpe* was closely associated with IS*1469* independent of where it was encoded, as this insertion sequence was detected exclusively in all *cpe*-encoding genomes (100%; **Fig. 4A-B**).

Accessory genome virulence potentials

The 110 strain *C. perfringens* pangenome consisted of 6 219 genes (including NCTC8239; **Fig. S2**); 1 965 core genes (31.5%), and 4 254 accessory genes (68.5%); with ~30-40% genes in any individual strain encoded within the accessory genome, potentially driving evolution and genome restructuring. Mobile genetic elements including plasmids, genomic islands and prophages could potentially contribute to virulence, given the plasticity of the genome. To explore this in more detail, we further analysed the accessory genomes, comparing different sub-sets of *C. perfringens* isolates. We first identified subset-specific genes using a bacterial pan-GWAS approach, with these genes further annotated based on NCBI RefSeq gene annotations and categorised under COG classes into three comparison groups: (1) CH vs FP; (2) FP outbreaks; (3) FP lineage I, FP lineage II-VII and CH-FP plasmid-CPE isolates (**Fig. S3A-C**).

Phosphotransferase system (PTS)-related genes (n=4) were encoded exclusively in CH isolates (present in 26/35 CH isolates; **Fig. S3A and Table S11**). These genes may contribute

359 to the isolates' fitness to utilise complex carbohydrates (COG category G) in competitive
360 niches, like the gastrointestinal tract (76). PTS genes have been linked to virulence regulation
361 in other pathogens including foodborne pathogen *Listeria monocytogenes* (77). Heat-shock
362 protein (Hsp70) DnaK co-chaperone was annotated in FP-specific accessory genome (present
363 in 57/74 FP isolates), which may be involved in capsule and pili formation which may
364 facilitate host colonisation (78-80).

365 Accessory genes specific to each FP outbreaks were variable (**Fig. S3B-C and Table S12**),
366 but 3 annotated functional classes were conserved; L (replication, recombination & repair), M
367 (cell wall/membrane/envelope biogenesis) and V (defense mechanisms). Prominent genes
368 detected in all isolates included phage-related proteins (n=49) (L, M and S),
369 glycosyltransferases (n=37) (M), restriction modification systems (n=16) (V), transposases
370 (n=9) (L) and integrases (n=8) (L). It was evident that most genes were associated with
371 phages, seemingly a major source of mobile genetic transfer.

372 Correspondingly, less group-specific accessory genes where present compared with other
373 isolates in lineages II-VII (**Fig. S3C and Table S13**). Notably, multidrug transporter 'small
374 multidrug resistance' genes were exclusively detected in FP lineage I isolates, whereas ABC
375 transporters were more commonly encoded in plasmid-carrying isolates (virulence plasmids
376 pCPF5603 and pCPF4969 carry various ABC transporter genes). The Mate efflux family
377 protein gene was detected solely in lineage II-VII isolates.

378 **Prophage genomes linked to enhanced *C. perfringens* fitness**

379 Phage are important drivers of bacterial evolution and adaptation, and presence of prophage
380 within bacterial genomes is often associated with enhanced survival and virulence e.g.
381 sporulation capacity and toxin secretion (81-83). Thus, mining phages in foodborne *C.*
382 *perfringens* genomes could reveal insights into the role of bacteriophage in modulating

diversity and pathogenesis traits (25). We identified through PHASTER a total of 7 prophages in all 109 genomes (**Fig. S4A-B**). Further exploration into virulence and survival-enhancing genes (**Fig. S4C**) encoded in these predicted prophage regions revealed the presence of virulence-related enzyme sialidase NanH (promotes colonisation), putative enterotoxin EntB, various ABC transporters (linked to multidrug resistance) and toxin-linked phage lysis holin (probable link to toxin secretion)(61, 84-86). No differences in number of prophages carried were detected between CH and FP isolates (**Fig. S4D-E**). These data suggested that phages could potentially contribute to increased accessory virulence within the genomes of food-poisoning associated *C. perfringens*, and indicates further research, using both experimental and genomic approaches, is required.

Discussion

C. perfringens is often associated with self-limiting or longer-term gastroenteritis, however our knowledge on the genomic components that may link to disease symptoms or epidemiological comparisons between outbreaks is limited. In this study, WGS data and in-depth genomic analysis on a representative sub-set of 109 gastrointestinal outbreak-associated *C. perfringens* isolates, revealed potential epidemic phylogenetic clusters linked to plasmid carriage, and specific virulence determinants, which were strongly associated with outbreak isolates.

In the context of disease control it is important to gain detailed genomic information to predict transmission modes for pathogens. Our analysis of care home isolates indicated a specific persistent clone may have been responsible for up to 9 individual gastrointestinal outbreaks in North East England over the 2013-2017 period, which represents the majority reported gastroenteritis outbreaks (>80%) in this area (10). Interestingly, a previous study

407 indicated presence of persistent identical *C. perfringens* genotypes within care home settings,
408 with several individuals harbouring identical strains (as determined via PFGE profiling)
409 throughout a 9-month sampling period, however none of these isolates were positive for
410 the *cpe* gene (87). Furthermore, although care home isolates were defined as 'non-foodborne'
411 according to local epidemiological investigations as no food samples were identified as *C.*
412 *perfringens*-positive, these outbreaks may have resulted from contaminated food products not
413 sampled. Indeed, a recent investigation into fresh meat products (>200 samples)
414 demonstrated significant contamination; beef (~30%), poultry and pork (both ~26%), with
415 90% of strains *cpe*-positive, suggesting food chain(s) or farmed animals as potential
416 reservoirs of enterotoxigenic *C. perfringens* (70, 88). Interestingly, 18% prevalence of *cpe*-
417 positive *C. perfringens* strains had previously been reported in food handlers' faeces
418 (confirmed via PCR), denoting a potential role of the human reservoir in outbreaks (89).
419 Determination of these potential reservoirs in the spread of *cpe*-positive *C. perfringens* to at-
420 risk populations would necessitate a One Health approach, and large-scale WGS-based
421 screening to ascertain the phylogenomics of strains isolated from diverse sources surrounding
422 outbreak-linked vicinities.

423 Successful colonisation of invading *C. perfringens* is required for efficient toxin production,
424 which ultimately leads to gastrointestinal symptoms. Through computational analysis we
425 determined that plasmid-*cpe* (specifically plasmids pCPF4969 and pCPF5603) carrying
426 strains predominated within both non-foodborne and food-poisoning outbreak-related *C.*
427 *perfringens* isolates (~82%). These two virulence plasmids, pCPF4969 and pCPF5603,
428 encoded several important virulence genes including ABC transporter and adhesin (also
429 known as collagen adhesion gene *cna*) that could contribute to enhanced survival and
430 colonisation potential of *C. perfringens* within the gastrointestinal tract (90). Plasmid
431 pCPF4969 also contained a putative bacteriocin gene that may allow *C. perfringens* to

outcompete other resident microbiota members, and thus overgrow and cause disease in the gut environment (73). Plasmid pCPF5603 encoded important toxin genes *cpe* and *cpb2*, plus additional toxins, many of which are linked to food poisoning symptoms, such as diarrhoea and cramping.

Interestingly, 4 out of 109 outbreak-associated strains were *cpe*-negative, suggesting secondary virulence genes (e.g. *pfo* and *cpb2*) may be associated with *C. perfringens*-associated gastroenteritis. A recent WGS-based study on FP *C. perfringens* outbreaks in France determined that ~30% of isolates were *cpe*-negative (13/42) (26), indicating this gene may not be the sole virulence determinant linked to *C. perfringens* gastroenteritis. Although we observed less *cpe*-negative strains in our collection in comparison to this study, this may be due to our targeted *cpe*-positive isolation strategy (standard practice at PHE). Thus, to determine the importance and diversity of *cpe*-negative strains in FP outbreaks this will require untargeted isolation schemes in the future.

Typical *C. perfringens*-associated food poisoning was previously thought to be primarily caused by chromosomal-*cpe* strains. This is linked to their phenotypic capacity to withstand high temperatures (via production of a protective small acid soluble protein), and high salt concentrations during the cooking process, in addition to the shorter generation time, when compared to plasmid-*cpe* carrying strains (68, 91). Previous studies have indicated that these strains commonly assemble into distinct clusters that lack the *pfo* gene, which we also noted in the FP lineage I data from this study (26, 92-94). Nevertheless, plasmid-borne *cpe*-carrying strains (pCPF4969 or pCPF5603) have also been associated with previous food poisoning outbreaks, with a previous study indicating that pCPF5603-carrying strains (encoding IS*1151*) were associated with food poisoning in Japanese nursing homes (7 out of 9 isolates) (71). However, these plasmid-*cpe* outbreaks have been described as a relatively uncommon occurrence, thus it is surprising that our findings indicate that most outbreak isolated strains

457 (81.6%; 89/109) carried a *cpe*-plasmid (60, 67). The fact that plasmid-*cpe* strains can cause
458 diverse symptoms including short-lived food poisoning, and long-lasting non-foodborne
459 diarrhoea, implicates additional factors in disease pathogenesis. The gut microbiome may be
460 one such host factor as previous studies have reported that care home residents have a less
461 diverse and robust microbiota when compared to those residing in their own homes
462 (including individuals colonised with *C. perfringens*), and thus impaired 'colonisation
463 resistance' may mean certain *C. perfringens* strains can overcome these anti-infection
464 mechanisms and initiate disease pathogenesis (64, 87, 95).

465 Chromosomal-*cpe* is reported to be encoded on a transposon-like element Tn*5565* (6.3 kb,
466 with flanking copies of IS*1470*), which can form an independent and stable circular-form in
467 culture extracts (losing both copies of IS*1470*) (72, 74). This transposition element TN*5565*
468 was commonly thought to be integrated into the chromosome at a specific site as a unit. The
469 fact that our computational analysis failed to detect any *cpe*, IS*1469* (*cpe*-specific), and
470 IS*1470* (Tn*5565*-specific) in the high-sequencing-coverage PH029 genome (317X
471 sequencing depth/coverage) indicates that Tn*5565* can be lost or may be passed on to other *C.*
472 *perfringens* cells. However, it should be noted that flanking IS*1470* of Tn*5565* may not have
473 been correctly assembled during the genome assembly process due to the repetitive nature of
474 those sequences (short-read sequencing).

475 As WGS provides enhanced resolution to identify outbreak-specific clonal strains, our study
476 highlighted the importance of implementing WGS for *C. perfringens* profiling in reference
477 laboratories, in place of the conventional fAFLP (92, 93, 96). Routine *C. perfringens*
478 surveillance of the care home environment and staff could prove critical for vulnerable
479 populations, as outbreaks could rapidly spread, and this approach could potentially pinpoint
480 the sources of contamination, and eventually eliminate persistent *cpe*-strains in the
481 environment (87). In light of the potential rapid transmissibility of *C. perfringens cpe*-strains

482 responsible for food-poisoning outbreaks, real-time portable sequencing approaches such as
483 the MinION, could facilitate the rapid identification of outbreak strains, which has been
484 recently been reported to identify outbreak *Salmonella* strains in <2h (97, 98).

485 Our data highlights the genotypic and epidemiology relatedness of a large collection of *C.*
486 *perfringens* strains isolated from food poisoning cases from across England and Wales, and
487 indicates potential circulation of disease-associated strains, and the potential impact of
488 plasmid-associated-*cpe* dissemination, linked to outbreak cases. This study indicates that
489 further WGS phylogenetic and surveillance studies of diversely-sourced *C. perfringens*
490 isolates are required for us to fully understand the potential reservoir of food poisoning-
491 associated strains, so that intervention or prevention measures can be devised to prevent the
492 spread of epidemiologically important genotypes, particularly in vulnerable communities,
493 including older adults residing in care homes.

494

495 Electronic supplemental materials

496 Supplementary Figure S1

497 Supplementary Figure S2

498 Supplementary Figure S3

499 Supplementary Figure S4

500 Supplementary Table S1

501 Supplementary Table S2

502 Supplementary Table S3

503 Supplementary Table S4

Supplementary Table S5

Supplementary Table S6

Supplementary Table S7

Supplementary Table S8

Supplementary Table S9

Supplementary Table S10

Supplementary Table S11

Supplementary Table S12

Supplementary Table S13

Acknowledgments

This work was supported by a Wellcome Trust Investigator Award (100974/C/13/Z), and the Biotechnology and Biological Sciences Research Council (BBSRC); Institute Strategic Programme Gut Microbes and Health BB/R012490/1, and its constituent project(s) BBS/E/F/000PR10353 and BBS/E/F/000PR10356, and Institute Strategic Programme Gut Health and Food Safety BB/J004529/1 to LJH, and Institute Strategic Programme Microbes in the Food Chain BB/R012504/1 to AEM. This research was supported in part by the NBI Computing infrastructure for Science (CiS) group through the provision of a High-Performance Computing (HPC) Cluster. We also thank Dr. Andrew Page (Quadram Institute, UK) for the helpful discussion on computational analysis.

R.K., C.A. and L.J.H. designed the study. R.K. and A.P. processed the sequencing data. R.K. performed the genomic analysis and graphed the figures. S.C. and A. P. provided essential assistance in genome assembly and genomic analysis. A.M. contributed in genomic analysis

tools and edited the manuscript, R.K., C.A. and L.J.H. analysed the data and co-wrote the manuscript. CS and CA managed the culture collection, genotyping, clinical data collection, and processed samples for sequencing.

References

1. Awad MM, Ellemor DM, Boyd RL, Emmins JJ, Rood JI. Synergistic effects of alpha-toxin and perfringolysin O in Clostridium perfringens-mediated gas gangrene. Infect Immun. 2001;69:7904-10.
2. Kiu R, Hall LJ. An update on the human and animal enteric pathogen *Clostridium perfringens*. Emerging Microbes & Infections. 2018;7(1):141.
3. Kiu R, Caim S, Alexander S, Pachori P, Hall LJ. Probing Genomic Aspects of the Multi-Host Pathogen *Clostridium perfringens* Reveals Significant Pangenome Diversity, and a Diverse Array of Virulence Factors. Front Microbiol. 2017;8:2485.
4. Revitt-Mills SA, Rood JI, Adams V. Clostridium perfringens extracellular toxins and enzymes: 20 and counting. Microbiology Australia. 2015:114-7.
5. Kim YJ, Kim SH, Ahn J, Cho S, Kim D, Kim K, et al. Prevalence of Clostridium perfringens toxin in patients suspected of having antibiotic-associated diarrhea. Anaerobe. 2017;48:34-6.
6. Sim K, Shaw AG, Randell P, Cox MJ, McClure ZE, Li MS, et al. Dysbiosis anticipating necrotizing enterocolitis in very premature infants. Clin Infect Dis. 2015;60(3):389-97.
7. Hobbs BC, Smith ME, Oakley CL, Warrack GH, Cruickshank JC. Clostridium welchii food poisoning. J Hyg (Lond). 1953;51(1):75-101.
8. DuPont HL. Clinical practice. Bacterial diarrhea. N Engl J Med. 2009;361(16):1560-9.
9. O'Brien SJ, Larose TL, Adak GK, Evans MR, Tam CC, Foodborne Disease Attribution Study G. Modelling study to estimate the health burden of foodborne diseases: cases, general practice consultations and hospitalisations in the UK, 2009. BMJ Open. 2016;6(9):e011119.
10. Dolan GP, Foster K, Lawler J, Amar C, Swift C, Aird H, et al. An epidemiological review of gastrointestinal outbreaks associated with Clostridium perfringens, North East of England, 2012-2014. Epidemiol Infect. 2016;144(7):1386-93.
11. Adak GK, Long SM, O'Brien SJ. Trends in indigenous foodborne disease and deaths, England and Wales: 1992 to 2000. Gut. 2002;51(6):832-41.
12. Tam CC, Rodrigues LC, Viviani L, Dodds JP, Evans MR, Hunter PR, et al. Longitudinal study of infectious intestinal disease in the UK (IID2 study): incidence in the community and presenting to general practice. Gut. 2012;61(1):69-77.
13. Borriello SP, Larson HE, Welch AR, Barclay F, Stringer MF, Bartholomew BA. Enterotoxigenic Clostridium perfringens: a possible cause of antibiotic-associated diarrhoea. Lancet. 1984;1(8372):305-7.
14. Larson HE, Borriello SP. Infectious diarrhea due to Clostridium perfringens. J Infect Dis. 1988;157(2):390-1.
15. Food Standards Agency. Foodborne Disease Strategy 2010-2015. 2011 May 2011.

16. Food Standards Agency. Report of the study of infectious intestinal disease in England. Commun Dis Rep CDR Wkly. 2000;10(51):457.
17. Rood JI, Adams V, Lacey J, Lyras D, McClane BA, Melville SB, et al. Expansion of the *Clostridium perfringens* toxin-based typing scheme. Anaerobe. 2018.
18. Fernandez Miyakawa ME, Pistone Creydt V, Uzal FA, McClane BA, Ibarra C. Clostridium perfringens enterotoxin damages the human intestine in vitro. Infect Immun. 2005;73(12):8407-10.
19. Shinoda T, Shinya N, Ito K, Ohsawa N, Terada T, Hirata K, et al. Structural basis for disruption of claudin assembly in tight junctions by an enterotoxin. Sci Rep. 2016;6:33632.
20. Ronco T, Stegger M, Ng KL, Lilje B, Lyhs U, Andersen PS, et al. Genome analysis of Clostridium perfringens isolates from healthy and necrotic enteritis infected chickens and turkeys. BMC Res Notes. 2017;10(1):270.
21. Li C, Yan X, Lillehoj HS. Complete Genome Sequence of Clostridium perfringens LLY_N11, a Necrotic Enteritis-Inducing Strain Isolated from a Healthy Chicken Intestine. Genome Announc. 2017;5(44).
22. Gaucher ML, Perron GG, Arsenault J, Letellier A, Boulianne M, Quessy S. Recurring Necrotic Enteritis Outbreaks in Commercial Broiler Chicken Flocks Strongly Influence Toxin Gene Carriage and Species Richness in the Resident Clostridium perfringens Population. Front Microbiol. 2017;8:881.
23. Park JY, Kim S, Oh JY, Kim HR, Jang I, Lee HS, et al. Characterization of Clostridium perfringens isolates obtained from 2010 to 2012 from chickens with necrotic enteritis in Korea. Poultry Science. 2015;94(6):1158-64.
24. Verherstraeten S, Goossens E, Valgaeren B, Pardon B, Timbermont L, Vermeulen K, et al. The synergistics necrohemorrhagic action of Clostridium perfringens perfringolysin and alpha toxin in the bovine intestine and against bovine endothelial cells. Vet Res. 2013;44:45.
25. Lacey JA, Allnutt TR, Vezina B, Van TTH, Stent T, Han X, et al. Whole genome analysis reveals the diversity and evolutionary relationships between necrotic enteritis-causing strains of Clostridium perfringens. BMC Genomics. 2018;19(1):379.
26. Mahamat Abdelrahim A, Radomski N, Delannoy S, Djellal S, Le Négrate M, Hadjab K, et al. Large-Scale Genomic Analyses and Toxinotyping of Clostridium perfringens Implicated in Foodborne Outbreaks in France. 2019;10(777).
27. Amar CF, East CL, Grant KA, Gray J, Iturriza-Gomara M, Maclure EA, et al. Detection of viral, bacterial, and parasitological RNA or DNA of nine intestinal pathogens in fecal samples archived as part of the english infectious intestinal disease study: assessment of the stability of target nucleic acid. Diagn Mol Pathol. 2005;14(2):90-6.
28. Roussel S, Felix B, Grant K, Dao TT, Brisabois A, Amar C. Fluorescence amplified fragment length polymorphism compared to pulsed field gel electrophoresis for Listeria monocytogenes subtyping. BMC Microbiol. 2013;13:14.
29. Saitoh Y, Suzuki H, Tani K, Nishikawa K, Irie K, Ogura Y, et al. Strucutral insight into tight junction disassembly by *Clostridium perfringens* enterotoxin. Science. 2015;347(6223):775-8.
30. Bankevich A, Nurk S, Antipov D, Gurevich AA, Dvorkin M, Kulikov AS, et al. SPAdes: a new genome assembly algorithm and its applications to single-cell sequencing. J Comput Biol. 2012;19(5):455-77.
31. Page AJ, De Silva N, Hunt M, Quail MA, Parkhill J, Harris SR, et al. Robust high-throughput prokaryote de novo assembly and improvement pipeline for Illumina data. Microb Genom. 2016;2(8):e000083.
32. Boetzer M, Henkel CV, Jansen HJ, Butler D, Pirovano W. Scaffolding pre-assembled contigs using SSPACE. Bioinformatics. 2011;27(4):578-9.

617 33. Nadalin F, Vezzi F, Policriti A. GapFiller: a de novo assembly approach to fill the gap
618 within paired reads. BMC Bioinformatics. 2012;13 Suppl 14:S8.
619 34. Seemann T. Prokka: rapid prokaryotic genome annotation. Bioinformatics.
620 2014;30(14):2068-9.
621 35. Davis MP, van Dongen S, Abreu-Goodger C, Bartonicek N, Enright AJ. Kraken: a set
622 of tools for quality control and analysis of high-throughput sequence data. Methods.
623 2013;63(1):41-9.
624 36. Pritchard L, Glover RH, Humphris S, Elphinstone JG, Toth IK. Genomics and
625 taxonomy in diagnostics for food security: soft-rotting enterobacterial plant pathogens.
626 Analytical Methods. 2016;8(1):12-24.
627 37. Koren S, Walenz BP, Berlin K, Miller JR, Bergman NH, Phillippy AM. Canu:
628 scalable and accurate long-read assembly via adaptive k-mer weighting and repeat separation.
629 Genome Res. 2017;27(5):722-36.
630 38. Page AJ, Cummins CA, Hunt M, Wong VK, Reuter S, Holden MT, et al. Roary: rapid
631 large-scale prokaryote pan genome analysis. Bioinformatics. 2015;31(22):3691-3.
632 39. Katoh K, Standley DM. MAFFT Multiple Sequence Alignment Software Version 7:
633 Improvements in Performance and Usability. Mol Biol Evol. 2013;30(4):772-80.
634 40. Page AJ, Taylor B, Delaney AJ, Soares J, Seemann T, Keane JA, et al. SNP-sites:
635 rapid efficient extraction of SNPs from multi-FASTA alignments. Microb Genom.
636 2016;2(4):e000056.
637 41. Price MN, Dehal PS, Arkin AP. FastTree 2--approximately maximum-likelihood trees
638 for large alignments. PLoS One. 2010;5(3):e9490.
639 42. Letunic I, Bork P. Interactive tree of life (iTOL) v3: an online tool for the display and
640 annotation of phylogenetic and other trees. Nucleic Acids Res. 2016;44(W1):W242-5.
641 43. Seemann T, Klotzl F, Page AJ. snp-dists. 0.2 ed2018. p. Convert a FASTA alignment
642 to SNP distance matrix.
643 44. Cheng L, Connor TR, Siren J, Aanensen DM, Corander J. Hierarchical and spatially
644 explicit clustering of DNA sequences with BAPS software. Mol Biol Evol. 2013;30(5):1224-
645 8.
646 45. Tonkin-Hill G, John A. L, Stephen D. B, Simon D. W. F, Jukka C. RhierBAPS: An R
647 Implementation of the Population Clustering Algorithm hierBAPS. Wellcome Open Research.
648 2018;3(July):93.
649 46. Hadfield J, Croucher NJ, Goater RJ, Abudahab K, Aanensen DM, Harris SR.
650 Phandango: an interactive viewer for bacterial population genomics. Bioinformatics. 2017.
651 47. Jia B, Raphenya AR, Alcock B, Waglechner N, Guo P, Tsang KK, et al. CARD 2017:
652 expansion and model-centric curation of the comprehensive antibiotic resistance database.
653 Nucleic Acids Res. 2017;45(D1):D566-D73.
654 48. Seemann T. ABRicate. 0.5 ed2018. p. Mass screening of contigs for antimicrobial
655 resistance or virulence genes.
656 49. Hunt M, Mather AE, Sanchez-Buso L, Page AJ, Parkhill J, Keane JA, et al. ARIBA:
657 rapid antimicrobial resistance genotyping directly from sequencing reads. Microb Genom.
658 2017;3(10):e000131.
659 50. R Development Core Team. R: A language and environment for statistical computing.
660 Vienna, Austria2010. Available from: http://www.R-project.org/.
661 51. Warnes GR, Bolker B, Bonebakker L, Gentleman R, Huber W, Liaw A, et al. gplots:
662 Various R Programming Tools for Plotting Data. R package version 3.0.1 ed2016.
663 52. Roosaare M, Puustusmaa M, Mols M, Vaher M, Remm M. PlasmidSeeker:
664 identification of known plasmids from bacterial whole genome sequencing reads. PeerJ.
665 2018;6:e4588.

666 53. Brynildsrud O, Bohlin J, Scheffer L, Eldholm V. Rapid scoring of genes in microbial
667 pan-genome-wide association studies with Scoary. Genome Biology. 2016;17.
668 54. Huerta-Cepas J, Szklarczyk D, Forslund K, Cook H, Heller D, Walter MC, et al.
669 eggNOG 4.5: a hierarchical orthology framework with improved functional annotations for
670 eukaryotic, prokaryotic and viral sequences. Nucleic Acids Res. 2016;44(D1):D286-93.
671 55. Huerta-Cepas J, Forslund K, Pedro Coelho L, Szklarczyk D, Juhl Jensen L, von
672 Mering C, et al. Fast genome-wide functional annotation through orthology assignment by
673 eggNOG-mapper. Mol Biol Evol. 2017.
674 56. Arndt D, Marcu A, Liang Y, Wishart DS. PHAST, PHASTER and PHASTEST:
675 Tools for finding prophage in bacterial genomes. Brief Bioinform. 2017.
676 57. Rutherford K, Parkhill J, Crook J, Horsnell T, Rice P, Rajandream MA, et al. Artemis:
677 sequence visualization and annotation. Bioinformatics. 2000;16(10):944-5.
678 58. Sullivan MJ, Petty NK, Beatson SA. Easyfig: a genome comparison visualizer.
679 Bioinformatics. 2011;27(7):1009-10.
680 59. Amar C. Fluorescent amplified fragment length polymorphism (fAFLP) analysis of
681 Listeria monocytogenes. Methods Mol Biol. 2014;1157:95-101.
682 60. Lahti P, Heikinheimo A, Johansson T, Korkeala H. Clostrdium perfringens type A
683 strains carrying a plasmid-borne enterotoxin gene (Genotype IS1151-cpe or IS1470-like-cpe)
684 as a common cause of food poisoning. J Clin Microbiol. 2008;46(1):371-3.
685 61. Li J, McClane BA. Contributions of NanI sialidase to Caco-2 cell adherence by
686 Clostridium perfringens type A and C strains causing human intestinal disease. Infect Immun.
687 2014;82(11):4620-30.
688 62. Theoret JR, Li J, Navarro MA, Garcia JP, Uzal FA, McClane BA. Native or
689 Proteolytically Activated NanI Sialidase Enhances the Binding and Cytotoxic Activity of
690 Clostridium perfringens Enterotoxin and Beta Toxin. Infect Immun. 2018;86(1).
691 63. Osman KM, Elhariri M. Antibiotic resistance of Clostridium perfringens isolates from
692 broiler chickens in Egypt. Rev Sci Tech. 2013;32(3):841-50.
693 64. Larcombe S, Hutton ML, Lyras D. Involvement of Bacteria Other Than Clostridium
694 difficile in Antibiotic-Associated Diarrhoea. Trends Microbiol. 2016;24(6):463-76.
695 65. Fisher DJ, Miyamoto K, Harrison B, Akimoto S, Sarker MR, McClane BA.
696 Association of beta2 toxin production with Clostridium perfringens type A human
697 gastrointestinal disease isolates carrying a plasmid enterotoxin gene. Mol Microbiol.
698 2005;56(3):747-62.
699 66. Sparks SG, Carman RJ, Sarker MR, McClane BA. Genotyping of enterotoxigenic
700 Clostridium perfringens fecal isolates associated with antibiotic-associated diarrhea and food
701 poisoning in North America. J Clin Microbiol. 2001;39(3):883-8.
702 67. Tanaka D, Isobe J, Hosorogi S, Kimata K, Shimizu M, Katori K, et al. An outbreak of
703 food-borne gastroenteritis caused by Clostridium perfringens carrying the cpe gene on a
704 plasmid. Japanese Journal of Infectious Diseases. 2003;56(3):137-9.
705 68. Li J, McClane BA. Further comparison of temperature effects on growth and survival
706 of Clostridium perfringens type A isolates carrying a chromosomal or plasmid-borne
707 enterotoxin gene. Appl Environ Microbiol. 2006;72(7):4561-8.
708 69. Collie RE, McClane BA. Evidence that the enterotoxin gene can be episomal in
709 Clostridium perfringens isolates associated with non-food-borne human gastrointestinal
710 diseases. J Clin Microbiol. 1998;36(1):30-6.
711 70. Lindstrom M, Heikinheimo A, Lahti P, Korkeala H. Novel insights into the
712 epidemiology of Clostridium perfringens type A food poisoning. Food Microbiol.
713 2011;28(2):192-8.
714 71. Tanaka D, Kimata K, Shimizu M, Isobe J, Watahiki M, Karasawa T, et al.
715 Genotyping of Clostridium perfringens isolates collected from food poisoning outbreaks and

716 healthy individuals in Japan based on the cpe locus. Japanese Journal of Infectious Diseases.
717 2007;60(1):68-9.
718 72. Cornillot E, Saint-Joanis B, Daube G, Katayama S, Granum PE, Canard B, et al. The
719 enterotoxin gene (cpe) of Clostridium perfringens can be chromosomal or plasmid-borne.
720 Mol Microbiol. 1995;15(4):639-47.
721 73. Miyamoto K, Fisher DJ, Li J, Sayeed S, Akimoto S, McClane BA. Complete
722 sequencing and diversity analysis of the enterotoxin-encoding plasmids in Clostridium
723 perfringens type A non-food-borne human gastrointestinal disease isolates. J Bacteriol.
724 2006;188(4):1585-98.
725 74. Brynestad S, Sarker MR, McClane BA, Granum PE, Rood JI. Enterotoxin plasmid
726 from Clostridium perfringens is conjugative. Infect Immun. 2001;69(5):3483-7.
727 75. Miyamoto K, Li JH, McClane BA. Enterotoxigenic Clostridium perfringens:
728 Detection and Identification. Microbes Environ. 2012;27(4):343-9.
729 76. Gera K, Le T, Jamin R, Eichenbaum Z, McIver KS. The phosphoenolpyruvate
730 phosphotransferase system in group A Streptococcus acts to reduce streptolysin S activity and
731 lesion severity during soft tissue infection. Infect Immun. 2014;82(3):1192-204.
732 77. Mertins S, Joseph B, Goetz M, Ecke R, Seidel G, Sprehe M, et al. Interference of
733 components of the phosphoenolpyruvate phosphotransferase system with the central
734 virulence gene regulator PrfA of Listeria monocytogenes. J Bacteriol. 2007;189(2):473-90.
735 78. Genevaux P, Wawrzynow A, Zylicz M, Georgopoulos C, Kelley WL. DjlA is a third
736 DnaK co-chaperone of Escherichia coli, and DjlA-mediated induction of colanic acid capsule
737 requires DjlA-DnaK interaction. J Biol Chem. 2001;276(11):7906-12.
738 79. Barocchi MA, Ries J, Zogaj X, Hemsley C, Albiger B, Kanth A, et al. A
739 pneumococcal pilus influences virulence and host inflammatory responses. Proc Natl Acad
740 Sci U S A. 2006;103(8):2857-62.
741 80. Arita-Morioka K, Yamanaka K, Mizunoe Y, Ogura T, Sugimoto S. Novel strategy for
742 biofilm inhibition by using small molecules targeting molecular chaperone DnaK.
743 Antimicrob Agents Chemother. 2015;59(1):633-41.
744 81. Boyd EF. Bacteriophage-encoded bacterial virulence factors and phage-pathogenicity
745 island interactions. Adv Virus Res. 2012;82:91-118.
746 82. Kinney DM, Bramucci MG. Analysis of Bacillus subtilis sporulation with spore-
747 converting bacteriophage PMB12. J Bacteriol. 1981;145(3):1281-5.
748 83. Fortier LC, Sekulovic O. Importance of prophages to evolution and virulence of
749 bacterial pathogens. Virulence. 2013;4(5):354-65.
750 84. Shimizu T, Ohtani K, Hirakawa H, Ohshima K, Yamashita A, Shiba T, et al.
751 Complete genome sequence of Clostridium perfringens, an anaerobic flesh-eater. Proc Natl
752 Acad Sci U S A. 2002;99(2):996-1001.
753 85. Andersen JL, He GX, Kakarla P, K CR, Kumar S, Lakra WS, et al. Multidrug efflux
754 pumps from Enterobacteriaceae, Vibrio cholerae and Staphylococcus aureus bacterial food
755 pathogens. Int J Environ Res Public Health. 2015;12(2):1487-547.
756 86. Govind R, Dupuy B. Secretion of Clostridium difficile toxins A and B requires the
757 holin-like protein TcdE. PLoS Pathog. 2012;8(6):e1002727.
758 87. Lakshminarayanan B, Harris HM, Coakley M, O'Sullivan O, Stanton C, Pruteanu M,
759 et al. Prevalence and characterization of Clostridium perfringens from the faecal microbiota
760 of elderly Irish subjects. J Med Microbiol. 2013;62(Pt 3):457-66.
761 88. Hu WS, Kim H, Koo OK. Molecular genotyping, biofilm formation and antibiotic
762 resistance of enterotoxigenic Clostridium perfringens isolated from meat supplied to school
763 cafeterias in South Korea. Anaerobe. 2018;52:115-21.

764 89. Heikinheimo A, Lindstrom M, Granum PE, Korkeala H. Humans as reservoir for
765 enterotoxin gene--carrying Clostridium perfringens type A. Emerg Infect Dis.
766 2006;12(11):1724-9.
767 90. Miyamoto K, Yumine N, Mimura K, Nagahama M, Li J, McClane BA, et al.
768 Identification of novel Clostridium perfringens type E strains that carry an iota toxin plasmid
769 with a functional enterotoxin gene. PLoS One. 2011;6(5):e20376.
770 91. Li J, McClane BA. A novel small acid soluble protein variant is important for spore
771 resistance of most Clostridium perfringens food poisoning isolates. PLoS Pathog.
772 2008;4(5):e1000056.
773 92. Ashton PM, Nair S, Peters TM, Bale JA, Powell DG, Painset A, et al. Identification of
774 Salmonella for public health surveillance using whole genome sequencing. PeerJ.
775 2016;4:e1752.
776 93. Schmid D, Allerberger F, Huhulescu S, Pietzka A, Amar C, Kleta S, et al. Whole
777 genome sequencing as a tool to investigate a cluster of seven cases of listeriosis in Austria
778 and Germany, 2011-2013. Clin Microbiol Infect. 2014;20(5):431-6.
779 94. Deguchi A, Miyamoto K, Kuwahara T, Miki Y, Kaneko I, Li J, et al. Genetic
780 characterization of type A enterotoxigenic Clostridium perfringens strains. PLoS One.
781 2009;4(5):e5598.
782 95. Claesson MJ, Jeffery IB, Conde S, Power SE, O'Connor EM, Cusack S, et al. Gut
783 microbiota composition correlates with diet and health in the elderly. Nature.
784 2012;488(7410):178-84.
785 96. Keto-Timonen R, Heikinheimo A, Eerola E, Korkeala H. Identification of Clostridium
786 species and DNA fingerprinting of Clostridium perfringens by amplified fragment length
787 polymorphism analysis. J Clin Microbiol. 2006;44(11):4057-65.
788 97. Gardy J, Loman NJ, Rambaut A. Real-time digital pathogen surveillance - the time is
789 now. Genome Biol. 2015;16(1):155.
790 98. Quick J, Ashton P, Calus S, Chatt C, Gossain S, Hawker J, et al. Rapid draft
791 sequencing and real-time nanopore sequencing in a hospital outbreak of Salmonella. Genome
792 Biol. 2015;16:114.

793

794

Figure legends

Fig. 1 Population structure and sample distribution statistics for genome assemblies

(A) Population structure of 109 *C. perfringens* isolates analysed in this study. Mid-point rooted maximum-likelihood phylogeny inferred from 73 882 SNPs identified in 110 diarrhoea-associated *C. perfringens* isolates (including NCTC8239). The colour-coded rings indicated cohort-specific origins of isolates. Cluster VIII (green ring; clusters determined via hierBAPS clustering analysis) consists of primarily isolates obtained from multiple care home-associated outbreaks. Historical food poisoning isolate NCTC8239 was used as a public reference genome as indicated in the figure. Bootstrap values are represented in the tree. Branch lengths are indicative of the estimated nucleotide substitution per site (SNPs). **(B)** Temporal distribution of all 109 *C. perfringens* genomes included in this study. **(C)** Contig count distribution of *C. perfringens* genome assemblies in this study. More than 70% of the total assemblies are <200 contigs.

Fig. 2 Phylogenomic analysis of care home-associated *C. perfringens* isolates

(A) Mid-point rooted maximum-likelihood phylogeny inferred from 64 560 SNPs (in core gene alignment) identified in 35 care home-associated *C. perfringens* isolates. The colour strips indicate diarrhoea outbreaks, location of outbreaks and fAFLP types respectively corresponding to the isolates. Branch lengths are indicative of the estimated SNP distance. Lineages and sub-lineages were determined via hierBAPS (level 1 & 2) clustering analysis. NCTC8239, a food poisoning isolate, was used as a public reference genome in this tree. Bootstrapping values are represented on the tree. **(B)** Unrooted maximum-likelihood tree (inferred from 191 SNPs in 18 genomes) of a sub-lineage IVc (excluding three genetically distant Welsh isolates) showing SNP distances in between 18 North-East England-derived

819 isolates of individual outbreaks (labeled in locations and years, and SNP range in outbreaks;
820 branches are colour-coded corresponding to individual outbreaks). SNP distances between
821 branches are indicated in red numbers. **(C)** Pairwise within-outbreak core-SNP distance
822 between isolates. **(D)** Pairwise outside-sub-lineage (IVb vs IVc) SNP comparison between
823 isolates. Data: Mann-Whitney test. **** P<0.0001.

824

825 **Fig. 3 Phylogenomic analysis of 75 foodborne-associated *C. perfringens* isolates**

826 **(A)** Mid-point rooted maximum-likelihood phylogeny of food-poisoning *C. perfringens*
827 inferred from 70 613 SNPs (in core gene alignment) identified in 75 individual isolates.
828 NCTC8239, a food poisoning strain isolated in 1949 (encodes *cpe* gene) is a RefSeq public
829 reference genome. Lineages were determined via hierBAPS clustering analysis. Bootstrap
830 values are represented in the tree. **(B)** Unrooted maximum-likelihood tree inferred from 2 505
831 SNPs in lineage VII (31 isolates). Four distinct clusters are identified in different outbreaks
832 comprising genetically-similar strains (labeled in locations and years, and SNP range in
833 outbreaks; branches are colour-coded corresponding to outbreak labels). **(C)** Pairwise core-
834 SNP distance comparison in between isolates within outbreaks. **(D)** Pairwise core-SNP
835 comparisons of within-major-lineage isolates in between individual outbreaks. Lineage I:
836 outbreaks 1,4,13 and 14; Lineage IV: outbreaks 3 and 7; Lineage VII: outbreaks 2, 7 and 10.
837 Data: Kruskal-Wallis test; **** P<0.0001.

838

839 **Fig. 4 Full virulence profiles of *C. perfringens* isolates including virulence plasmids**

840 Binary heatmaps displaying presence and absence of toxin genes, AMR genes, plasmids,
841 plasmid-related sequences and *tcp* conjugative loci in corresponding isolates: **(A)** CH isolates
842 **(B)** FP isolates. Outbreaks were colour-coded according to the colour system in previous

figures. Coloured cells represent presence of genes and white cells represent absence of genes. Heatmaps were generated in R.

Fig. 5 Investigations on predicted plasmids carried by CH and FP isolates

(A) Comparative genomic visualisation of reference plasmids pCPF4969 and pCPF5603 with annotated features. **(B)** Genomic comparison of pCPF5603 reference plasmid and predicted plasmids from CH genomes. **(C)** Plasmid comparison in between pCPF4969 plasmid and FP-isolate predicted plasmids. **(D)** CPE-regions (Tn*5565*) extracted computationally from FP lineage I representative isolate genomes. **(E)** A computationally extracted 11-kbp region of NCTC8239 that encodes Tn5565 (including cpe and flanking IS1470 elements) compared to predicted Tn*5565* from PH004. Figures were produced using Easyfig v2.2.2.

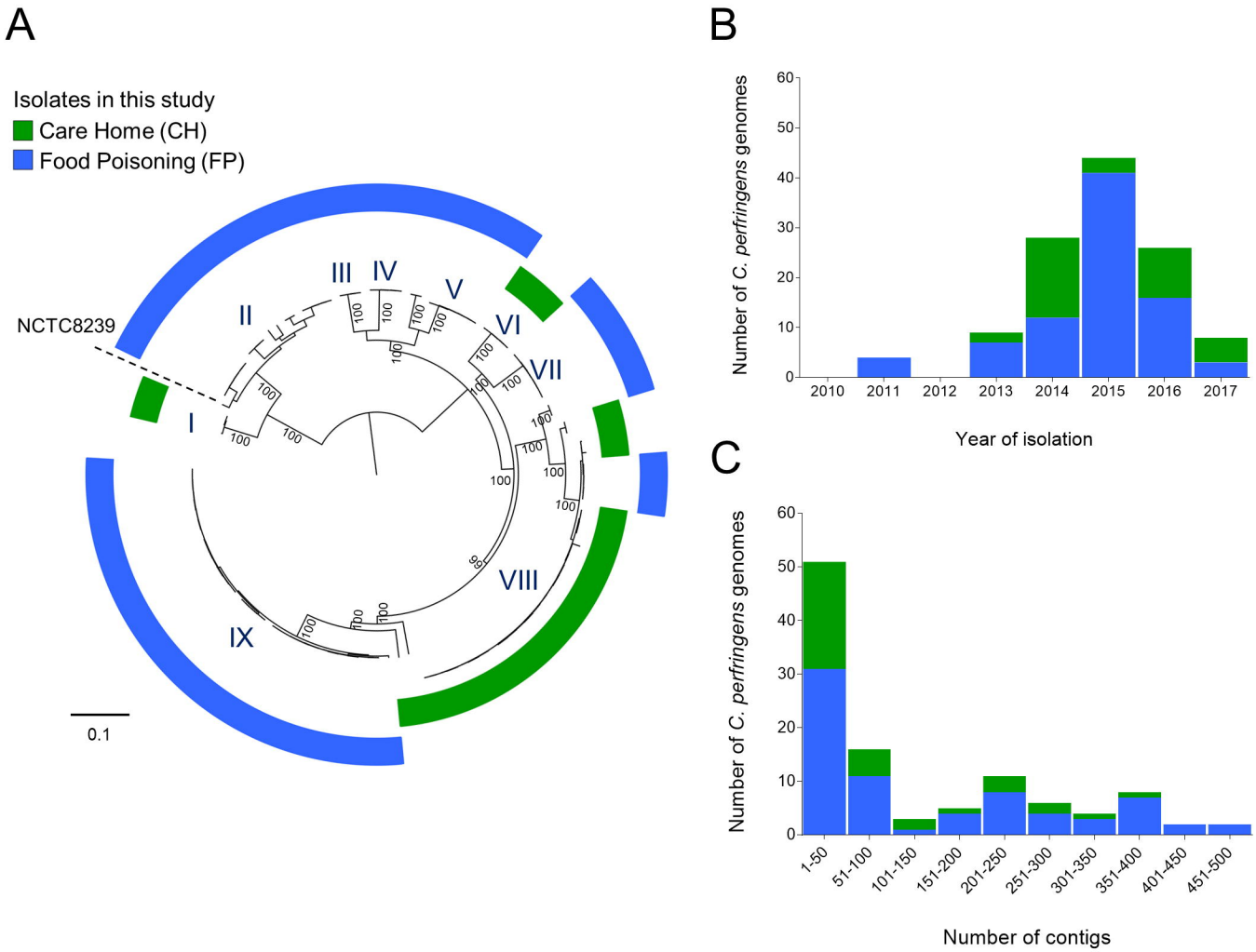

Fig. 1 Population structure and sample distribution statistics for genome assemblies
(A) Population structure of 109 *C. perfringens* isolates analysed in this study. Mid-point rooted maximum-likelihood phylogeny inferred from 73 882 SNPs identified in 110 diarrhoea-associated *C. perfringens* isolates (including NCTC8239). The colour-coded rings indicated cohort-specific origins of isolates. Cluster VIII (green ring; clusters determined via hierBAPS clustering analysis) consists of primarily isolates obtained from multiple care home-associated outbreaks. Historical food poisoning isolate NCTC8239 was used as a public reference genome as indicated in the figure. Bootstrap values are represented in the tree. Branch lengths are indicative of the estimated nucleotide substitution per site (SNPs). **(B)** Temporal distribution of all 109 *C. perfringens* genomes included in this study. **(C)** Contig count distribution of *C. perfringens* genome assemblies in this study. More than 70% of the total assemblies are <200 contigs.

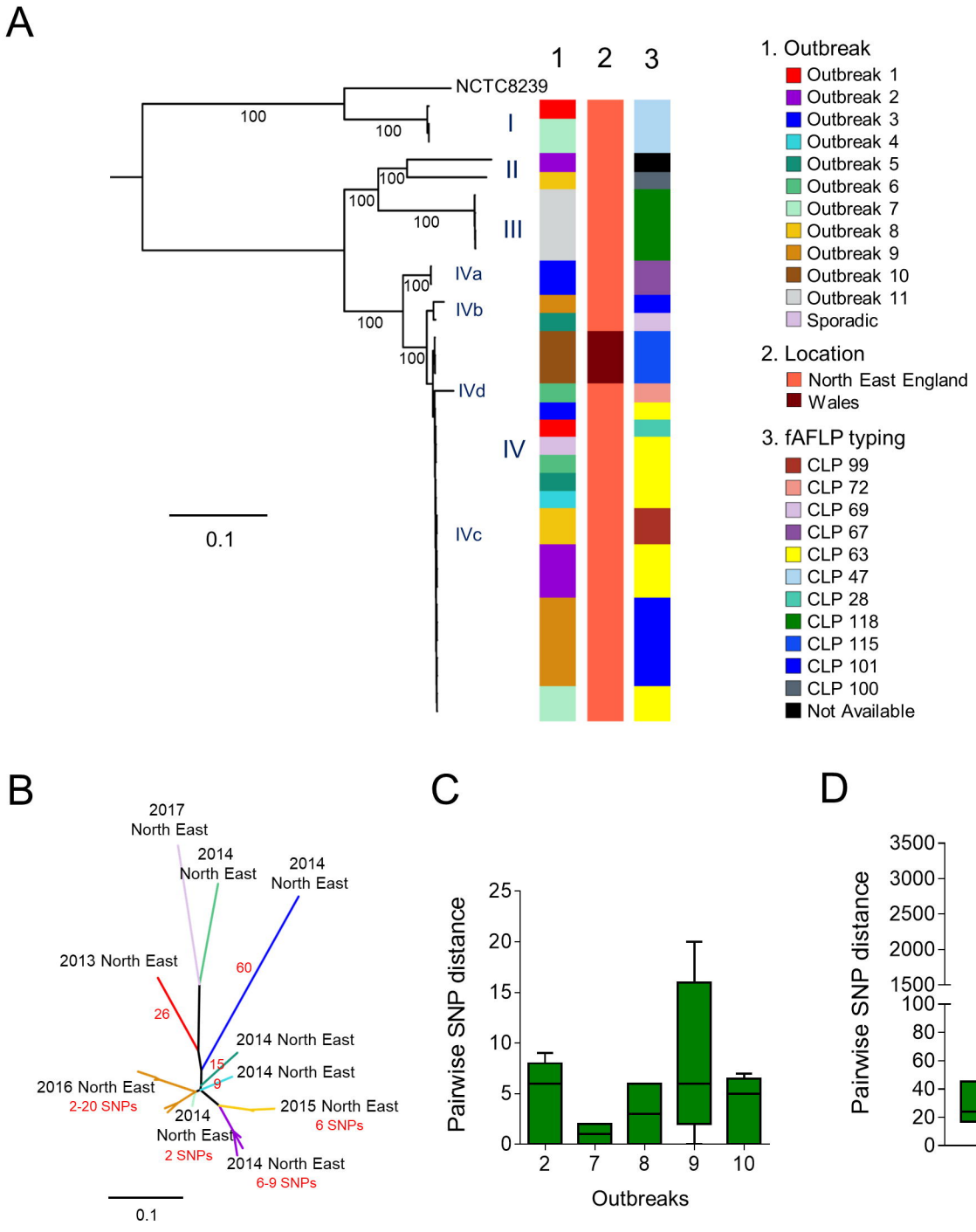

Fig. 2 Phylogenomic analysis of care home-associated *C. perfringens* isolates
(A) Mid-point rooted maximum-likelihood phylogeny inferred from 64 560 SNPs (in core gene alignment) identified in 35 care home-associated *C. perfringens* isolates. The colour strips indicate diarrhoea outbreaks, location of outbreaks and fAFLP types respectively corresponding to the isolates. Branch lengths are indicative of the estimated SNP distance. Lineages and sub-lineages were determined via hierBAPS (level 1 & 2) clustering analysis. NCTC8239, a food poisoning isolate, was used as a public reference genome in this tree. Bootstrapping values are represented on the tree. **(B)** Unrooted maximum-likelihood tree (inferred from 191 SNPs in 18 genomes) of a sub-lineage IVc showing SNP distances in between 18 North-East England-derived isolates of individual outbreaks (labeled in locations and years, and SNP range in outbreaks; branches are colour-coded corresponding to individual outbreaks). SNP distances between branches are indicated in red numbers. **(C)** Pairwise within-outbreak core-SNP distance between isolates. **(D)** Pairwise outside-sub-lineage (IVb vs IVc) SNP comparison between isolates. Data: Mann-Whitney test. **** P<0.0001.

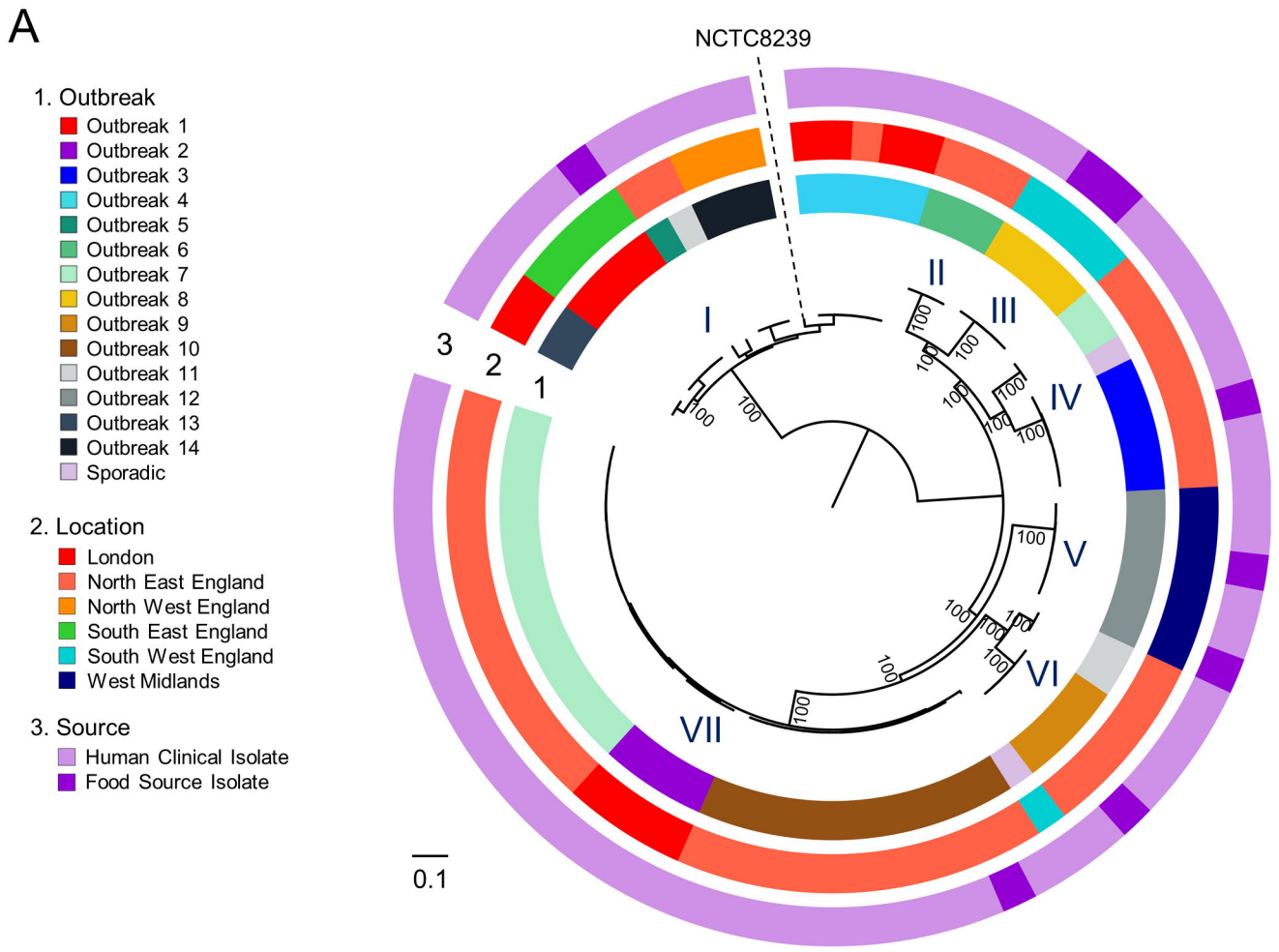

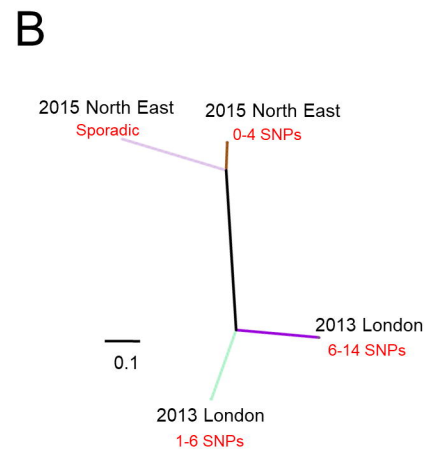

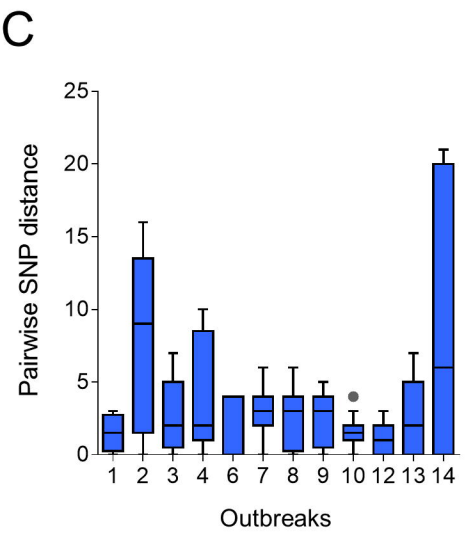

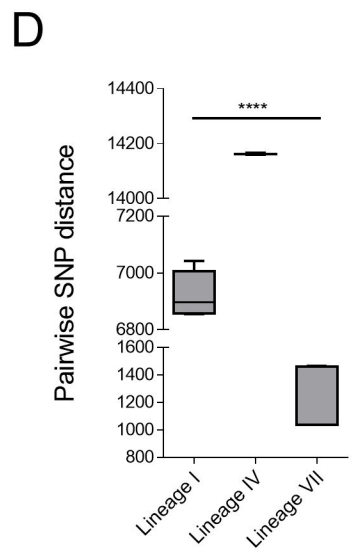

Fig. 3 Phylogenomic analysis of 75 foodborne-associated *C. perfringens* isolates
(A) Mid-point rooted maximum-likelihood phylogeny of food-poisoning *C. perfringens* inferred from 70 613 SNPs (in core gene alignment) identified in 75 individual isolates. NCTC8239, a food poisoning strain isolated in 1949 (encodes *cpe* gene) is a RefSeq public reference genome. Lineages were determined via hierBAPS clustering analysis. Bootstrap values are represented in the tree. **(B)** Unrooted maximum-likelihood tree inferred from 2 505 SNPs in lineage VII (31 isolates). Four distinct clusters are identified in different outbreaks comprising genetically-similar strains (labeled in locations and years, and SNP range in outbreaks; branches are colour-coded corresponding to outbreak labels). **(C)** Pairwise core-SNP distance comparison in between isolates within outbreaks. **(D)** Pairwise core-SNP comparisons of within-major-lineage isolates in between individual outbreaks. Lineage I: outbreaks 1,4,13 and 14; Lineage IV: outbreaks 3 and 7; Lineage VII: outbreaks 2, 7 and 10. Data: Kruskal-Wallis test; **** P<0.0001.

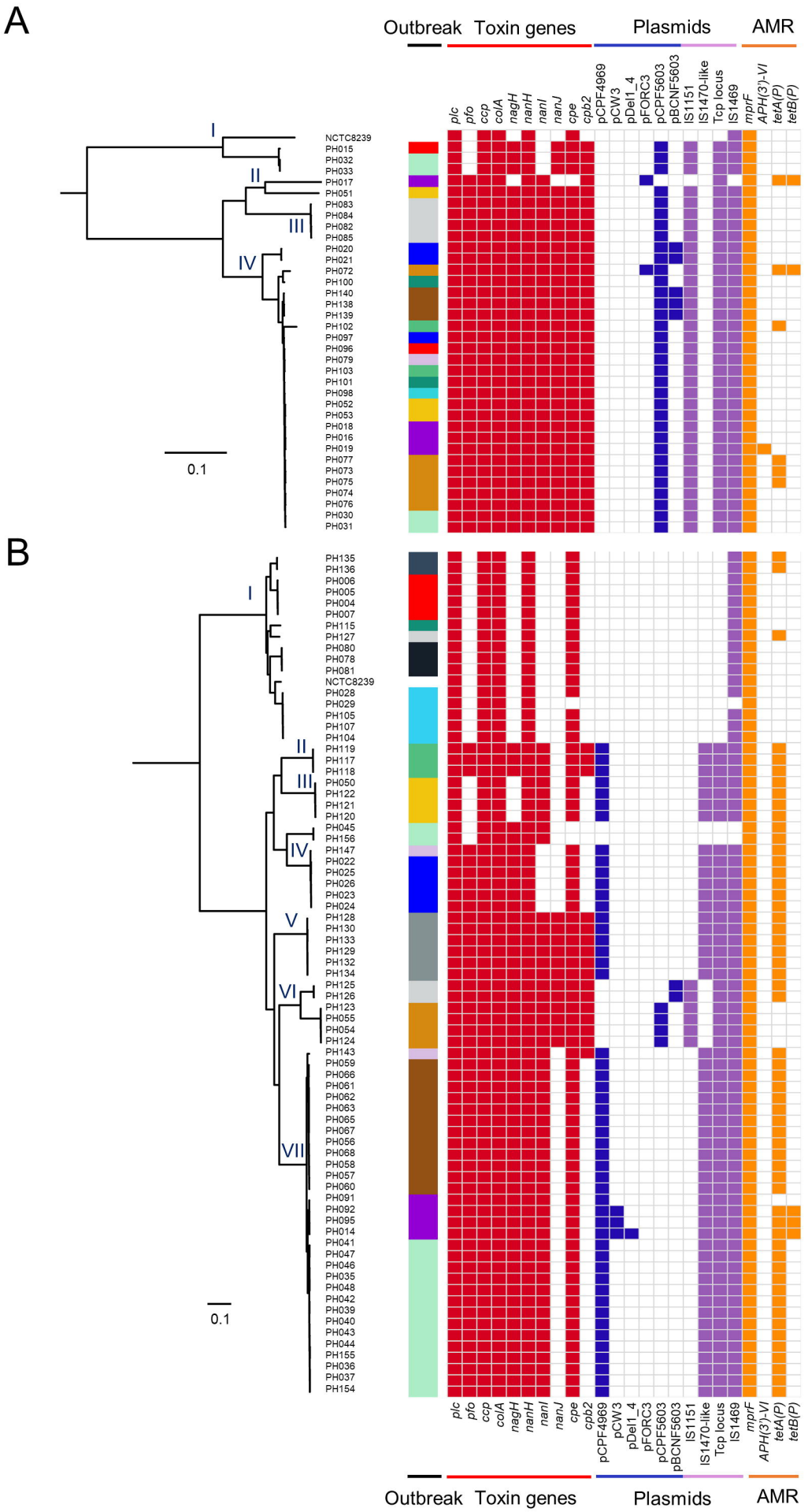

Fig. 5 Full virulence profiles of C. perfringens isolates including virulence plasmids
Binary heatmaps displaying presence and absence of toxin genes, AMR genes, plasmids, plasmid-related sequences and *tcp* conjugative loci in corresponding isolates: **(A)** CH isolates **(B)** FP isolates. Outbreaks were colour-coded according to the colour system in previous figures. Coloured cells represent presence of genes and white cells represent absence of genes. Heatmaps were generated in R.

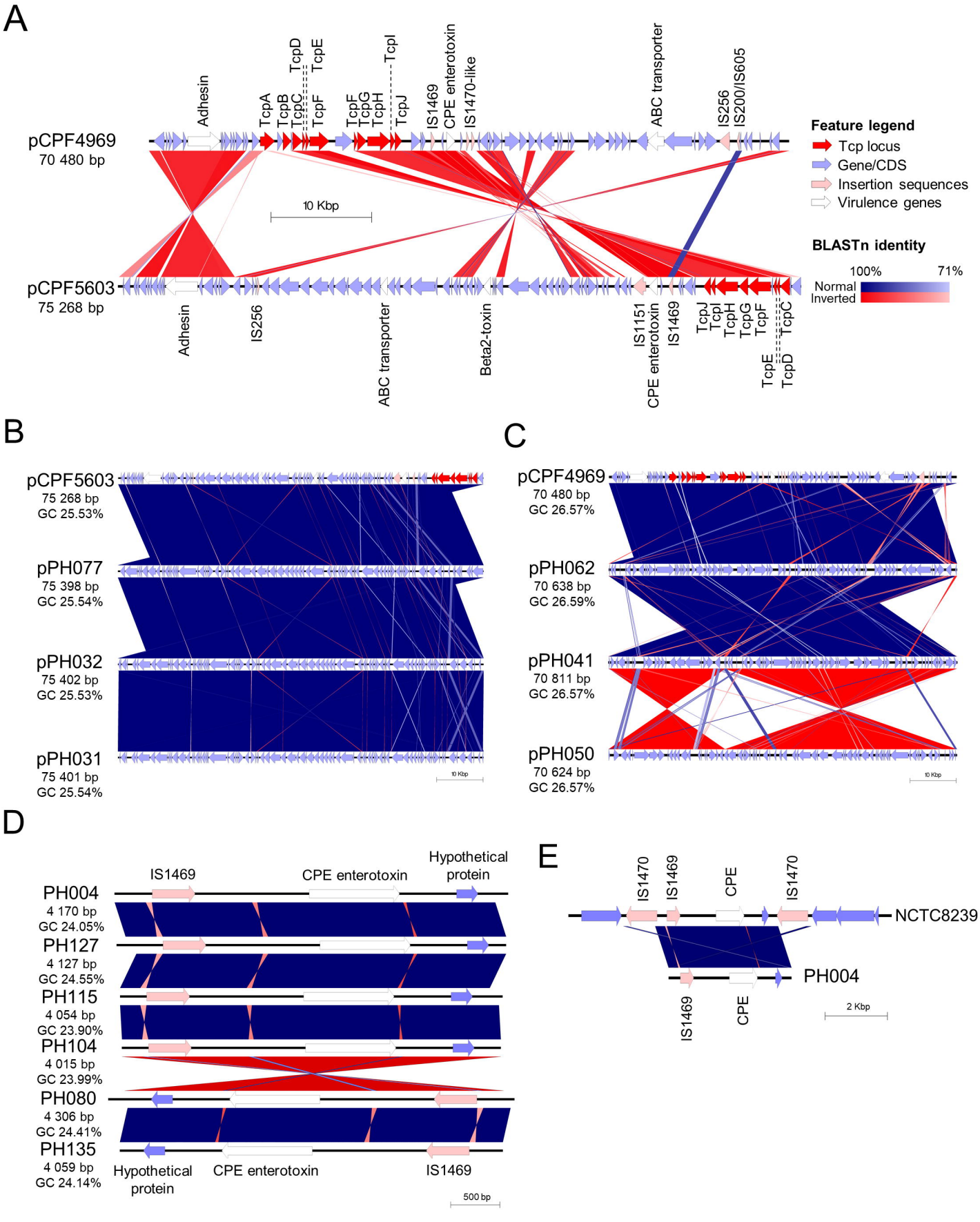

Fig. 5 Investigations on predicted plasmids carried by CH and FP isolates
(A) Comparative genomic visualisation of reference plasmids pCPF4969 and pCPF5603 with annotated features. **(B)** Genomic comparison of pCPF5603 reference plasmid and predicted plasmids from CH genomes. **(C)** Plasmid comparison in between pCPF4969 plasmid and FP-isolate predicted plasmids. **(D)** CPE-regions (Tn*5565*) extracted computationally from FP lineage I representative isolate genomes. **(E)** A computationally extracted 11-kbp region of NCTC8239 that encodes *Tn5565* (including *cpe* and flanking IS1470 elements) compared to predicted Tn*5565* from PH004. Figures were produced using Easyfig v2.2.2.